ISSN 1061-933X, Colloid Journal, 2017, Vol. 79, No. 1, pp. 26–34. © Pleiades Publishing, Ltd., 2017.
Original Russian Text © B.N. Galimzyanov, A.V. Mokshin, 2017, published in Kolloidnyi Zhurnal, 2017, Vol. 79, No. 1, pp. 16–24.

Surface Tension of Water Droplets upon Homogeneous Droplet Nucleation in Water Vapor

B. N. Galimzyanov[a], * and A. V. Mokshin[b]

[a] *Kazan (Volga Region) Federal University, ul. Kremlevskaya 18, Kazan, Tatarstan, 420008 Russia*
[b] *Landau Institute for Theoretical Physics, Russian Academy of Sciences, ul. Kosygina 2, Tatarstan, Moscow, 119334 Russia*
**e-mail: bulatgnmail@gmail.com*

Received June 9, 2016

Abstract—A method has been proposed for determining interfacial free energy from the data of molecular dynamics simulation. The method is based on the thermodynamic integration procedure and is distinguished by applicability to both planar interfaces and those characterized by a high curvature. The workability of the method has been demonstrated by the example of determining the surface tension for critical nuclei of water droplets upon condensation of water vapor. The calculation has been performed at temperatures of 273–373 K and a pressure of 1 atm, thus making it possible to determine the temperature dependence of the surface tension for water droplets and compare the results obtained with experimental data and the simulation results for a "planar" vapor–liquid interface.

DOI: 10.1134/S1061933X17010057

1. INTRODUCTION

According to the classical understandings [1], a first-order phase transition begins with the appearance of new phase nuclei. At the same time, size n of arising nuclei is of great importance. The term "size" implies the number of structural units (atoms, molecules, particles, etc.) that compose a nucleus. In accordance with the classical nucleation theory, nuclei are formed as a result of random fluctuations, but only nuclei with sizes larger than some critical size n_c can grow stably [2]. The formation of a new phase nucleus with a small (subcritical) size $n < n_c$ requires work, the majority of which is consumed for the formation of an interface between the nucleus and a mother phase. The work of the interface formation is referred to as "interfacial free energy" [1–3]. Thus, interfacial free energy is a key characteristic of nucleation, with this energy directly affecting both the latency period of the formation of a nucleus with the critical size and the nucleation rate, that is the term which characterizes the number of critical nuclei formed in unit volume of a system per unit time [1, 2, 4–9].

Direct experimental measurement of the interfacial free energy is a rather complex problem. On the other hand, the indirect estimation of this quantity on the basis of other measurable characteristics of nucleation (such as the critical nucleus size, nucleation rate, etc.) is, in the case of homogeneous nucleation in a bulk system, quite difficult as well [10], because only rather large nuclei, the sizes of which as a rule substantially exceed the critical size, can be detected in experiments. Moreover, adequate methods are unavailable for calculating the interfacial free energy of a surface characterized by a high curvature in the case of a very small object.

It should be noted that a significant progress has been achieved in the use of the classical molecular dynamics [11–17] and coarse-grained model interparticle interaction potentials for studying the properties and structural characteristics of water [18–21]. For example, Molinero and Moore were the first to show that a coarse-grained model of water can be employed to study water crystallization, with intermolecular interactions being described in this model by the modified Stillinger–Weber anisotropic potential [18, 19]. This modification of the Stillinger–Weber potential can be used to simulate the molecular dynamics of liquid and solid water due to the existence of a spatial-angle-dependent contribution that enables one to construct a tetrahedral structure, which is formed by hydrogen bonds in water [19, 22]. At the same time, this model has appeared to be able to restore the equation of state for water and to yield the values of different parameters, such as melting temperature, thermal conductivity, compressibility, density, enthalpy, and surface tension, more reliably than do the SPC/E and TIP4P atomistic models [18–20].

It will be shown in this work that the interfacial free energy can be calculated within the framework of the thermodynamic integration method on the basis of molecular dynamics simulation data. The calculations will be performed for homogeneous droplet nucle-

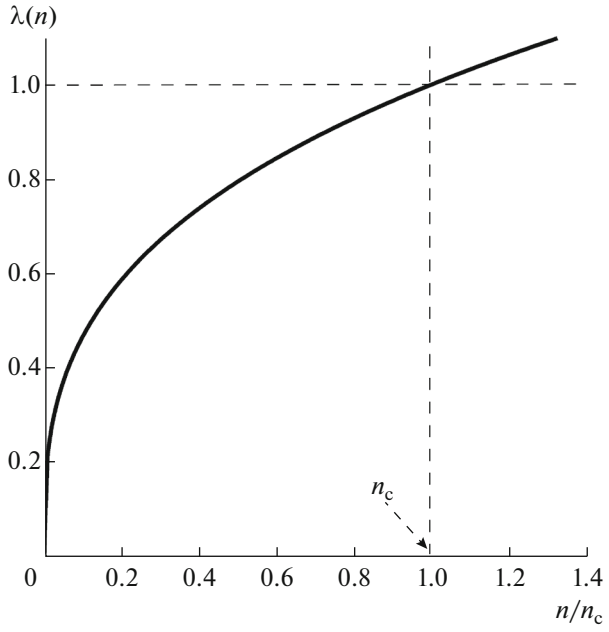

Fig. 1. Dependence of parameter λ on new phase nucleus size n.

ation in water vapor, where water droplets playing the role of new phase nuclei, and the interfacial free energy being related to their surface tension. Supersaturated water vapor will be considered at fixed temperatures lying in a range of 0–100°C and at the pressure $p = 1$ atm.

The work design is as follows. In the second section, the approach will be considered to the calculation of the interfacial free energy (surface tension) by means of the thermodynamic integration. This method will be discussed as applied to calculating the surface tension of critical water droplets at the vapor–liquid interface. In the third section, the details of the used simulation method will be described. The obtained results will be discussed in the fourth section. The obtained dependences of water surface tension on temperature and critical nucleus size will be presented, and the results will be compared with available experimental data and the results of molecular-dynamic simulations performed by other authors.

2. CALCULATION OF THE SURFACE TENSION FOR NUCLEI WITH CRITICAL SIZE

In the case of a two-phase system with a planar interface, the interfacial free energy may be determined by comparing the diagonal components of the pressure tensor, with these components being calculated using the Irving–Kirkwood microscopic expression [23, 24] and the Kirkwood–Buff approximation [5, 23, 25]. However, when a new phase is represented by a small compact nucleus, another approach must be used.

It is known that surface energy ω may be determined as excess energy per unit surface area [1]. In the case of a droplet occurring in a supersaturated vapor, the excess energy arises due to a lack of "neighbors" at surface particles as compared with particles occurring in a bulk phase. Confining ourselves to the consideration of neighbors at each particle within the first coordination sphere, we obtain the following relation [1]:

$$\omega = \frac{1}{2}u(\hat{r}_{ij})(z - z')n'. \quad (1)$$

Here, $\hat{r}_{ij}$ is the average distance between neighboring particles of a new phase; n' is the number of surface particles per unit surface area; z and z' are the first coordination numbers for bulk and surface particles, respectively.

Let us introduce the dimensionless parameter

$$\lambda = \left(\frac{n}{n_c}\right)^{1/3}, \quad (2)$$

which becomes equal to zero in the absence of new phase nuclei in a system and to unity when a nucleus (the largest one) reaches the critical size n_c. The dependence of the parameter λ on the nucleus size n is schematically represented in Fig. 1.

Since the surface energy depends on the nucleus size, its calculation by formula (1) yields a λ-dependence:

$$\omega = \omega(\lambda). \quad (3)$$

The surface tension may be determined directly by thermodynamic integration [20, 23, 24] as follows:

$$\sigma_s = -\int_{\lambda=0}^{\lambda=1} \left\langle \frac{\partial\omega(\lambda)}{\partial\lambda} \right\rangle_\lambda d\lambda. \quad (4)$$

Here, the denotation $\langle\ldots\rangle_\lambda$ implies averaging over an ensemble of independent trajectories $\partial\omega(\lambda)/\partial\lambda$ at a specific value of λ.

3. SIMULATION DETAILS

Molecular dynamics simulation is performed using the following Stillinger–Weber coarse-grained model potential adapted for water [19, 20, 26]:

$$U = \sum_{i,j}\phi_2(r_{ij}) + \sum_{i,j,k}\phi_3(r_{ij}, r_{ik}, \theta_{ijk}), \quad (5)$$

where the pair intermolecular interaction energy is determined by the contribution

$$\phi_2(r_{ij}) = A\varepsilon\left[B\left(\frac{\sigma}{r}\right)^p - 1\right]\exp\left(\frac{\sigma}{r_{ij} - r_{cut}}\right), \quad (6)$$

while the energy of the interaction between three molecules is described by the term

$$\phi_3(r_{ij}, r_{ik}, \theta_{ijk}) = \lambda\varepsilon\left[\cos\theta_{ijk} - \cos\theta_{0ijk}\right]^2 \times \exp\left(\frac{\gamma\sigma}{r_{ij} - r_{\text{cut}}}\right)\exp\left(\frac{\gamma\sigma}{r_{ik} - r_{\text{cut}}}\right). \quad (7)$$

Thus, the intermolecular interaction is directly taken into account in this anisotropic potential [26]. For water, the potential parameters have been found to take the following values [18, 19]: $A \approx 7.0495$, $B \approx 0.6022$, $p = 4$, $\lambda = 23.14$, $\gamma = 1.2$, and $\theta_{0ijk} = 109.47°$. At these values of the parameters, the Stillinger–Weber potential enables one to describe rather correctly the characteristics and physical properties of water in a temperature range of 273–350 K at the pressure $p = 1$ atm [18, 20]. Here, effective diameter of water molecule σ and potential well depth ε are 2.39 Å and 6.19 kcal/mol, respectively. Note that potential (5) is a short-range one with the cutoff radius $r_{\text{cut}} = 1.8\sigma$.

The system under simulation consists of $N = 8000$ identical molecules placed into a cubic cell, with periodic boundary conditions being used in the simulation. The classical equations of motion are integrated using the velocity Verlet algorithm with the time step $\Delta t = 1$ fs [27]. Initially, 100 independent samples are prepared at the temperature $T = 900$ K and the pressure $p = 1$ atm and equilibrated for 50 ps. Then, each sample is cooled at the rate $dT/dt = 10^{10}$ K/s to a required temperature lying in a range of 273–373 K and exposed at the constant pressure $p = 1$ atm for 10 ps. The temperature and pressure of the system are controlled using the Nose–Hoover thermostat and barostat, respectively [20, 27].

4. RESULTS

The affiliation of molecules to a liquid phase was identified using the Stillinger criterion [20, 28], according to which two molecules belong to the liquid phase when the distance between their centers is $r_j \le 1.5\sigma$, where $\sigma \approx 2.39$ Å corresponds to the position of the main maximum in the radial distribution function of molecules in liquid water [29, 30]. Figure 2 illustrates fragments of the simulation cell corresponding to water (water vapor) at $T = 273$ K and $p = 1$ atm at different time moments. For example, at time moment $t = 0.3$ ns, the system occurs in the vaporous state (Fig. 2a). In this case, the structural analysis shows no compact clusters that could be identified as liquid-phase nuclei. However, at $t = 0.8$ ns (Fig. 2b), such nuclei are already detected. Although the sizes of nuclei at this stage reach two or three tens of molecules, the nuclei are unstable and, as a rule, rapidly disappear. At time moment $t = 1.1$ ns, individual nuclei containing 70–80 molecules arise in the system. Note that the statistical interpretation of the curves for the growth of individual nuclei has revealed that $n \approx 75$ at $T = 273$ K and $p = 1$ atm corresponds to critical size n_c (Fig. 2c) [20]. Later, over a short period of time, these nuclei begin to grow rapidly due to both the attachment of individual molecules and the coalescence of the nuclei (Figs. 2d, 2e); by moment $t = 1.3$ ns, the system completely passes to the liquid state (Fig. 2f). A similar scenario of supersaturated vapor condensation is also observed at a higher temperature, although, as the temperature is elevated (in our case, this corresponds to a reduction in the level of the supersaturation), the time scale of the liquid–vapor transition enlarges.

Note that the scenario observed for the phase transition qualitatively corresponds to the classical concepts of condensation via the homogeneous nucleation mechanism [1, 2]. According to the classical nucleation theory, a stable growth of new phase nuclei is only possible after they reach a critical size. Indeed, as can be seen from Fig. 3, which presents the growth trajectory for the largest nucleus in the system at $T = 273$ K, at an initial stage, the size of the nucleus fluctuates in a certain range and begins to grow rapidly only after reaching the critical size $n_c \approx 75$ molecules. The critical size of the nucleus was found by the statistical method of inverse averaging of growth curves, which had been described detail in works [31, 32]. In order to estimate the n_c values for each considered (p, T)-state, the averaging was performed on the basis of results of the structural analysis for 100 independent samples. The obtained n_c values are listed in Table 1.

The surface tension of water droplets of the critical size was determined using the algorithm described in the second section. The calculations were performed on the basis of the data obtained for the largest (first) nucleus in the system. When forming this nucleus, the following values entering into relation (1) were found: potential energy $u(\hat{r}_{ij})$ per molecule of the new (liquid) phase; the number of molecules n' of the nucleus per unit surface area; and the first coordination numbers z and z' for bulk and surface molecules of the nucleus, respectively. These data were used to calculate the $\omega(n)$ curve, which was, then, transformed (at a known value of the critical size) into the $\omega(\lambda)$ curve, where $\lambda = (n/n_c)^{1/3}$.

Figure 4a exhibits the curves $\omega(\lambda)$ of the surface energy plotted on the basis of the simulation results obtained for 15 independent samples. The samples, in turn, corresponded to a supersaturated vapor at $T = 273$ K and $p = 1$ atm. Figure 4a indicates that all $\omega(\lambda)$ curves have a feature in common: the absolute value of $\omega(\lambda)$ increases with reduced nucleus size λ. For each $\omega(\lambda)$ curve, the derivative $\partial\omega(\lambda)/\partial\lambda$ was numerically calculated in the range $\lambda \in [0;1]$; then, averaging was performed over the results obtained for

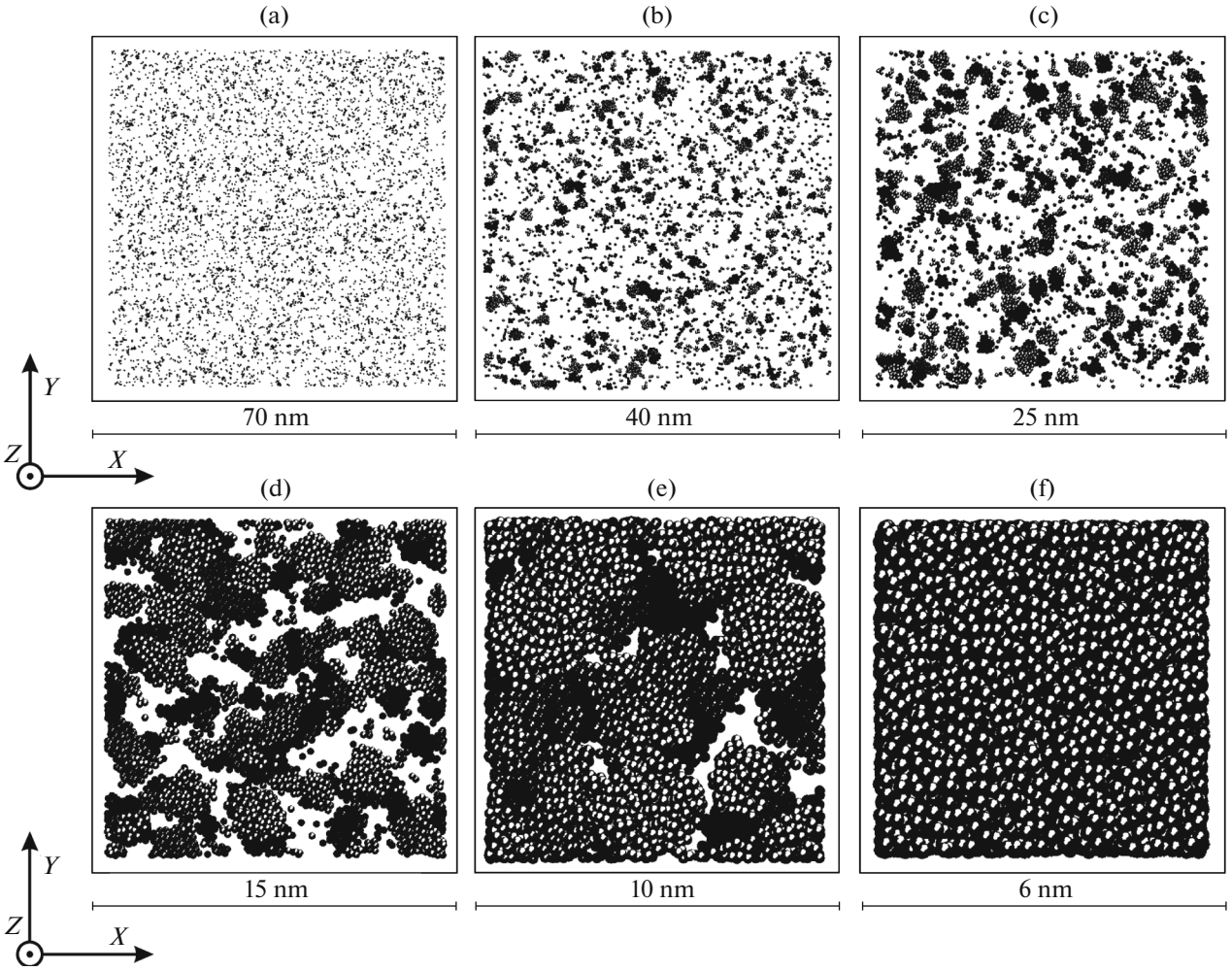

Fig. 2. Configurations of the studied system at different time moments: t = (a) 0.3, (b) 0.8, (c) 1.1, (d) 1.2, (e) 1.25, and (f) 1.3 ns. Temperature and pressure are $T = 273$ K and $p = 1$ atm, respectively.

100 independent samples. For example, Fig. 4b illustrates the averaged $\partial\omega(\lambda)/\partial\lambda$ curve obtained for the system at $T = 273$ K and $p = 1$ atm. In accordance with expression (4), the surface tension σ_s of a critically-sized nucleus is determined by the area a nucleus (water droplet) of the shaded region in the figure. Here, the critical size is $n_c \approx 75$ molecules. The values obtained for the surface tension coefficient σ_s at different temperatures are given in Table. 1.

As can be seen from Table 1, the critical nucleus size n_c and the surface tension of this nucleus (water droplet) at the liquid–vapor interface correspond to each temperature value. Moreover, the table presents nucleus surface areas S_f, which have been calculated under the condition that a nucleus is spherical, and the values of number density ρ, which determines the number of molecules per unit volume of a nucleus. Note that values of $\sigma_s(T)$ and $S_f(T)$ can be used to find the nucleation barrier $\Delta G_{n_c}(T)$ (the Gibbs free energy required to form a nucleus with a critical size n_c) within the framework of the classical nucleation theory as follows:

$$\Delta G_{n_c}(T) = \frac{1}{3}\sigma_s(T)S_f(T). \quad (8)$$

For the states corresponding to, e.g., $T = 273$ and 373 K, we obtain $\Delta G_{n_c}(T = 273\ \text{K}) = 30.6$ kcal/mol and $\Delta G_{n_c}(T = 373\ \text{K}) = 16.3$ kcal/mol, respectively.

The dependences presented in Fig. 5 attest to a correspondence between the values obtained for the critical nucleus size n_c and the surface tension σ_s. An increase of value of σ_s with the size n_c observed in the figure is quite expectable. Nevertheless, direct interpretation of this dependence with the use of the known Tolman relation [33–35], which takes into account the size-dependent correction to the surface tension, seems to be impossible, because each $\sigma_s(n_c)$ value pre-

sented in the figure corresponds to a specific temperature value.

Figure 6 shows the temperature dependences of the surface tension values obtained for nuclei of water droplets with the critical sizes in temperature range $T = 273–373$ K and at pressure $p = 1$ atm. In addition, the figure illustrates the experimental temperature dependences of the surface tension coefficient for a planar water–vapor interface [36–40], which are known to be adequately interpreted by the following expression:

$$\sigma_s(T) = c_1\left[1 - c_2\left(1 - \frac{T}{T_c}\right)\right]\left(1 - \frac{T}{T_c}\right)^m, \qquad (9)$$

where T_c is the critical temperature of water. The values of the parameters entering into Eq. (9) are listed in Table 2. Moreover, Fig. 6 shows temperature dependences $\sigma_s(T)$, which were obtained in [36, 38] within the frameworks of SPC/E, TIP3P, TIP3P/Ew, TIP3P/C, TIP4P, TIP4P/Ew, TIP4P/2005, TIP4P/Ice, TIP5P, and TIP6P atomistic model potentials. It should be noted that works [36, 38] report the values of σ_s for a planar liquid–vapor interface, where the surface tension was determined via the difference between the normal and tangential components of the pressure tensor in the surface layer of water.

In spite of the fact that the function $\sigma_s(T)$ can be adequately and quantitatively compared with experimental data and the results of calculations performed using the atomistic model potentials only taking into account the size effects (in this case, additional molecular dynamics calculations must be carried out for a planar interface), even the direct comparison leads to the following important conclusions.

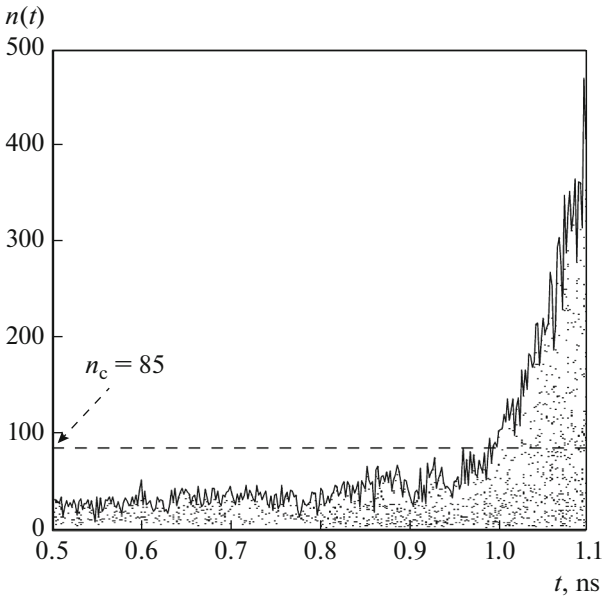

Fig. 3. Growth trajectory of the largest droplet in the system at $T = 273$ K and $p = 1$ atm.

Figure 6 indicates that the values of $\sigma_s(T)$ obtained for liquid phase (water) nuclei with critical sizes throughout the considered temperature range reproduce the experimental data for a planar interface.

Table 1. The values of characteristics for nuclei with critical sizes at different temperatures: n_c is the size, S_f is the surface area, ρ is the water numerical density, and σ_s is the surface tension calculated by expression (4); in parentheses are the experimental values [36–38]

T, K	n_c	S_f, 10^{-18} m^2	ρ, Å^{-3}	σ_s, 10^{-3} N/m
273	75 ± 25	8.30 ± 0.35	0.0333	76.9 ± 2.7 (75.6)
283	71 ± 27	8.31 ± 0.34	0.0333	73.1 ± 2.5 (72.8)
293	65 ± 27	7.56 ± 0.34	0.0333	73.1 ± 2.5 (72.8)
303	58 ± 22	7.02 ± 0.32	0.0332	72.2 ± 2.5 (71.2)
313	55 ± 21	6.79 ± 0.28	0.0331	71.1 ± 2.2 (69.6)
323	52 ± 18	6.56 ± 0.29	0.0329	69.1 ± 2.1 (67.9)
333	50 ± 15	6.41 ± 0.25	0.0328	67.6 ± 1.9 (66.2)
343	45 ± 13	5.99 ± 0.24	0.0326	65.5 ± 1.8 (64.5)
353	42 ± 12	5.75 ± 0.23	0.0324	64.9 ± 2.1 (62.7)
363	41 ± 12	5.68 ± 0.23	0.0322	62.2 ± 1.9 (60.8)
373	40 ± 10	5.62 ± 0.22	0.0319	60.1 ± 1.8 (58.9)

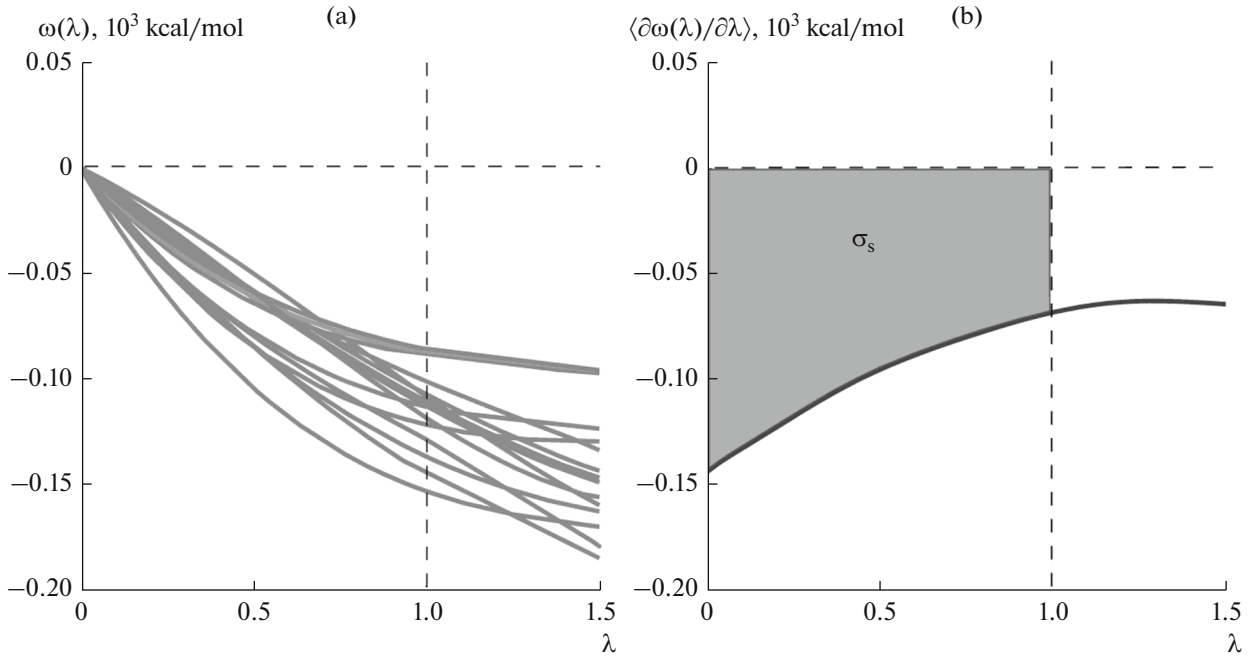

Fig. 4. Panel (a): $\omega(\lambda)$ curves obtained for 15 independent samples by molecular dynamics simulations of condensation of supersaturated water vapor at temperature $T = 273$ K and pressure $p = 1$ atm and panel (b): $\partial\omega(\lambda)/\partial\lambda$ curve resulting from averaging over 100 independent samples at $T = 273$ K and $p = 1$ atm. The area of the shaded region determines surface tension σ_s of a water droplet with the critical size $n_c \approx 75$ molecules.

At the same time, the data of $\sigma_s(T)$ obtained with atomistic model potentials of water are underestimated as compared to the experimental data (with the exception of the TIP4P/2005 and TIP4P/Ice models). Taking into account that the surface tension coefficient decreases as the curvature of the liquid–vapor interface increases (according to the Tolman formula [35] and its different modifications [33, 34]), it may be expected that the water model based on potential (5) may yield somewhat overestimated values of $\sigma_s(T)$. On the other hand, it is of interest that both our $\sigma_s(T)$ values and those calculated using atomistic model

Table 2. The values of parameters c_1, c_2, T_c, and m that correspond to the most adequate approximation by expression (9) of experimental data [37], results of this work, and those obtained for different models of water

System	c_1, 10^{-3} N/m	c_2	T_c, K	m
Experiment	236	0.625	647	1.256
This work	238 ± 15	0.628 ± 0.028	641 ± 22	1.222
SPC	139 ± 10	0.235 ± 0.021	621 ± 19	1.222
SPC/E	164 ± 11	0.312 ± 0.021	631 ± 23	1.222
TIP3P	140 ± 11	0.368 ± 0.018	619 ± 20	1.222
TIP3P/C	182 ± 10	0.725 ± 0.025	602 ± 18	1.222
TIP3P/Ew	157 ± 8	0.625 ± 0.025	612 ± 18	1.222
TIP4P	179 ± 11	0.484 ± 0.024	578 ± 19	1.222
TIP4P/Ew	182 ± 13	0.529 ± 0.026	638 ± 21	1.222
TIP4P/Ice	263 ± 6	0.695 ± 0.017	703 ± 22	1.222
TIP4P/2005	231 ± 8	0.656 ± 0.016	640 ± 19	1.222
TIP5P	139 ± 12	0.235 ± 0.019	594 ± 25	1.222
TIP6P	139 ± 13	0.221 ± 0.018	696 ± 24	1.222

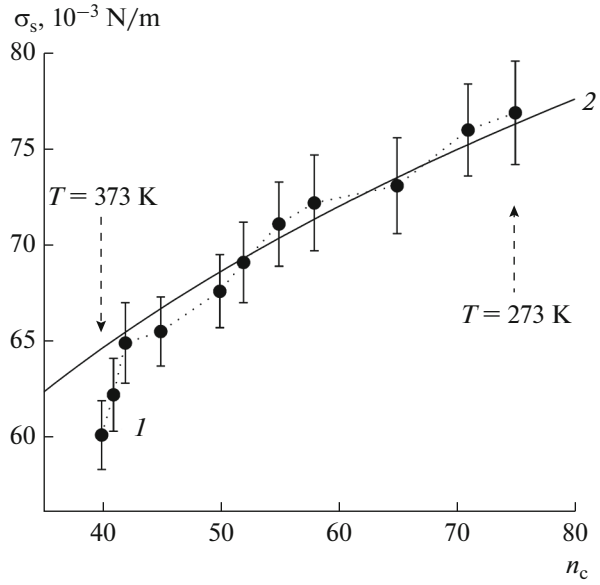

Fig. 5. Dependence of surface tension σ_s on critical size n_c of water nuclei: (*1*) data of numerical simulation, (*2*) approximation by the $\sigma_s(n_c) = \sigma_n[1 + 2(\delta_n/n_c)^{1/3}]^{-1}$ dependence at $\sigma_n \approx 0.343$ N/m and $\delta_n \approx 400$, which is identical to the Tolman formula [34, 35].

potentials are adequately approximated by expression (9). The approximated values of the parameters that enter into expression (9) are presented in Table 2. Finally, the good agreement between the data under consideration (see Fig. 6) directly attests to the efficiency of the method proposed in this work for determining the surface tension of small nuclei of liquid (droplets) and vapor (bubbles) phases.

5. CONCLUSIONS

Numerical simulation has been used to study phase transitions for rather a long time beginning from the groundbreaking work by Alder and Wainwright [41]. However, the determination of the phase transition characteristics using the data of simulation still encounters great difficulties because of the absence of clear algorithms that could be used for this purpose. Important parameters, such as interfacial energy and nucleation barrier, are among these characteristics. Works [13, 14, 17] are of great interest from this point of view. In those works, computer simulation was employed to determine the values of the parameters that govern nucleation in water vapor under different conditions, such as near critical temperatures and nucleation on electrically neutral and charged nanoparticles. In the cited works, the heterogeneous nucleation has mainly been considered, while homogeneous nucleation remains to be studied and is of great interest from the point of view of studying the peculiarities of the initial stage of the phase transition.

In this work, a method has been proposed for determining the interfacial free energy directly from data obtained by molecular dynamics simulation. This method is based on the so-called thermodynamic integration, which enables one to determine a *change* in the free energy of a system using a set of possible trajectories of the potential energy upon a change in a specified order parameter. The method makes it possible to calculate the interfacial free energy for an interface with an arbitrary geometry. This is of importance for, e.g., studying small nuclei of a new phase.

The developed method has been used to find the values of the surface tension coefficient for water droplets condensing in supersaturated water vapor at temperatures $T = 273-373$ K and pressure $p = 1$ atm. Calculations have been carried out using the data of molecular dynamics simulation of water, with the adapted Stillinger–Weber potential being employed as an effective intermolecular interaction potential. A relation has been found between the critical size of a water droplet and the surface tension. The temperature dependence obtained for the surface tension coefficient has been compared with experimental data and the results of simulation performed using different atomistic model potentials of water. It has been shown that the values obtained for the surface tension of water droplets reproduce the experimental data obtained for a planar interface.

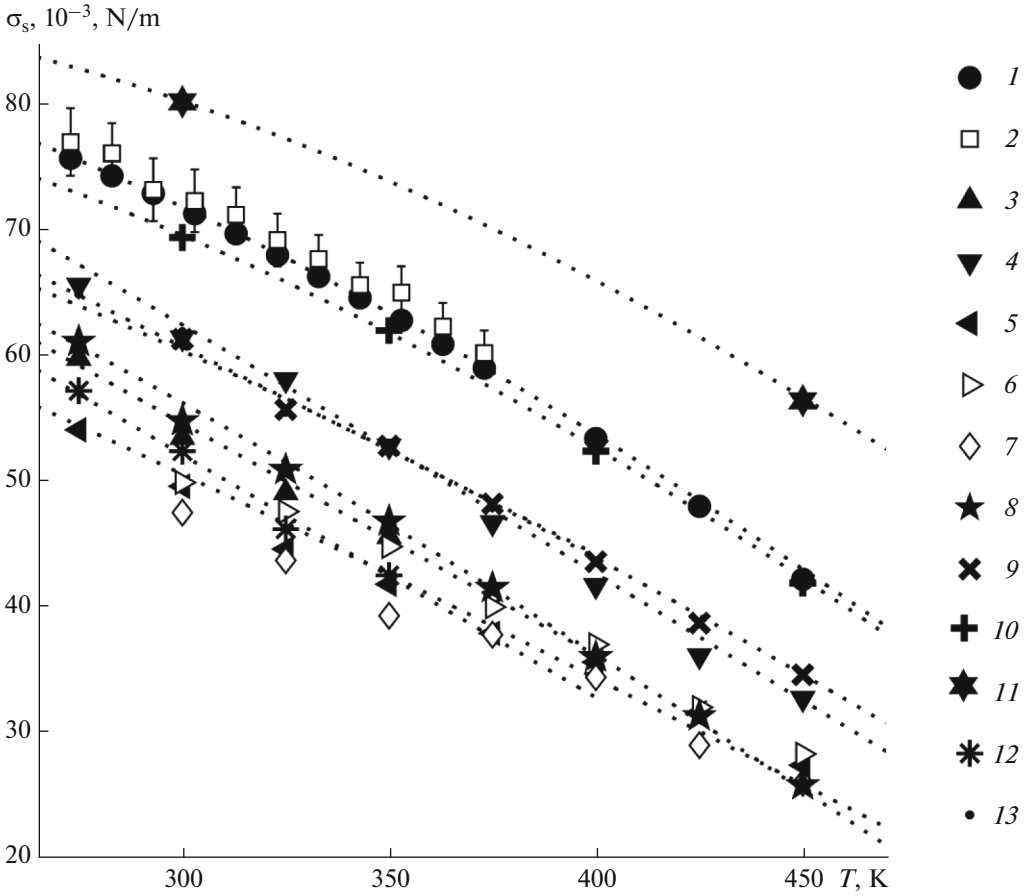

Fig. 6. Temperature dependences of water surface tension at pressure $p = 1$ atm: (*1*) experimental data [37], (*2*) results of this work, (*3*–*13*) data obtained for different model potentials: (*3*) SPC, (*4*) SPC/E, (*5*) TIP3P, (*6*) TIP3P/Ew, (*7*) TIP3P/C, (*8*) TIP4P, (*9*) TIP4P/Ew, (*10*) TIP4P/2005, (*11*) TIP4P/Ice, (*12*) TIP5P, and (*13*) TIP6P [36, 38]. Other markers denote the data taken from [36, 38–40] for different atomistic models.

ACKNOWLEDGMENTS

The molecular dynamics calculations have been carried out using the computer clusters of Kazan Federal University and the Joint Supercomputer Center of the Russian Academy of Sciences. The work was supported partly by a grant given to Kazan Federal University for fulfillment of a state assignment in the field of research.

REFERENCES

1. Frenkel', Ya.I., *Kineticheskaya teoriya zhidkostei* (Kinetic Theory of Liquids), Leningrad: Nauka, 1975.
2. Kashchiev, D., *Nucleation: Basic Theory with Applications*, Oxford: Butterworth-Heinemann, 2000.
3. Mokshin, A.V., *Teor. Mat. Fiz.*, 2015, vol. 183, p. 3.
4. Fokin, V.M., Zanotto, E.D., Yuritsyn, N.S., and Schmelzer, J.W.P., *J. Non-Cryst. Solids*, 2006, vol. 352, p. 2681.
5. Zubarev, D.N., *Neravnovesnaya statisticheskaya termodinamika* (Nonequilibrium Statistical Thermodynamics), Moscow: Mir, 1980.
6. Zubarev, D.N. and Morozov, V.G., *Statistical Mechanics of Nonequilibrium Processes. Vol. 1. Basic Concepts. Kinetic Theory*, Berlin: Academic, 1996.
7. Fokin, V.M., Zanotto, E.D., and Schmelzer, J.W.P., *J. Non-Cryst. Solids*, 2003, vol. 321, p. 52.
8. Tovbin, Yu.K., *Russ. J. Phys. Chem. A*, 2010, vol. 84, p. 1717.
9. Tovbin, Yu.K. and Rabinovich, A.B., *Izv. Akad. Nauk, Ser. Khim.*, 2010, vol. 4, p. 663.
10. Skripov, V.P., *Metastabil'naya zhidkost'* (Metastable Liquid), Moscow: Nauka, 1972.
11. Zheligovskaya, E.A. and Malenkov, G.G., *Zh. Strukt. Khim.*, 2005, vol. 46, p. 284.
12. Malenkov, G.G., *Zh. Strukt. Khim.*, 2006, vol. 47, p. 5.
13. Shevkunov, S.V., *Zh. Eksp. Teor. Fiz.*, 2009, vol. 136, p. 282.
14. Shevkunov, S.V., *Zh. Eksp. Teor. Fiz.,* 2009, vol. 135, p. 510.
15. Malenkov, G.G., *Colloid J.*, 2010, vol. 72, p. 653.
16. Malenkov, G.G., *Zh. Strukt. Khim.*, 2013, vol. 54, p. 258.
17. Shevkunov, S.V., *High Temperature*, 2013, vol. 51, p. 79.

18. Molinero, V. and Moore, E.B., *J. Phys. Chem. B*, 2009, vol. 113, p. 4008.
19. Moore, E.B. and Molinero, V., *Nature* (London), 2011, vol. 479, p. 506.
20. Mokshin, A.V. and Galimzyanov, B.N., *J. Phys. Chem. B*, 2012, vol. 116, p. 11959.
21. Zipoli, F., Laino, T., Stolz, S., Martin, E., Winkelmann, C., et al., *J. Chem. Phys.*, 2013, vol. 139, p. 094501.
22. Stanley, H.E. and Teixeira, J., *J. Chem. Phys.*, 1980, vol. 73, p. 3404.
23. Biscay, F., Ghoufi, A., Lachet, V., and Malfreyt, P., *J. Phys. Chem.*, 2011, vol. 115, p. 8670.
24. Irving, J.H. and Kirkwood, J.G., *J. Chem. Phys.*, 1950, vol. 18, p. 817.
25. Kirkwood, J.G. and Buff, F.P., *J. Chem. Phys.*, 1949, vol. 17, p. 338.
26. Stillinger, F. and Weber, T.A., *Phys. Rev. B*, 1985, vol. 31, p. 5262.
27. Frenkel, D. and Smit, B., *Understanding Molecular Simulation: From Algorithms to Applications*, San Diego: Academic, 2007.
28. Mokshin, A.V., Zabegaev, S.O., and Khusnutdinov, R.M., *Phys. Solid State*, 2011, vol. 53, p. 570.
29. Khusnutdinov, R.M. and Mokshin, A.V., *JETP Lett.*, 2014, vol. 100, p. 39.
30. Mokshin, A.V., Khusnutdinov, R.M., Novikov, A.G., Blagoveshchenskii, N.M., and Puchkov, A.V., *Zh. Eksp. Teor. Fiz.*, 2015, vol. 148, p. 947.
31. Mokshin, A.V. and Galimzyanov, B.N., *J. Chem. Phys.*, 2014, vol. 140, p. 024104.
32. Mokshin, A.V., Galimzyanov, B.N., and Barrat, J.-L., *Phys. Rev. E: Stat. Phys., Plasmas, Fluids, Relat. Interdiscip. Top.*, 2013, vol. 87, p. 062307.
33. Moody, M.P. and Attard, P., *Phys. Rev. Lett.*, 2013, vol. 91, p. 056104.
34. Schmelzer, J. and Mahnke, R., *J. Chem. Soc., Faraday Trans.*, 1986, vol. 82, p. 1413.
35. Tolman, R.S., *J. Chem. Phys.*, 1949, vol. 17, p. 333.
36. Vega, C. and De Miguel, E., *J. Chem. Phys.*, 2007, vol. 126, p. 154707.
37. White, H. and Sengers, J.V., Release on the Surface Tension of Ordinary Water Substance, Int. Association for the Properties of Water and Steam (IAPWS). *12 Int. Conf. on Properties of Water and Steam*, New York: Begell House, 1995.
38. Ismail, A.E., Grest, G.S., and Stevens, M.J., *J. Chem. Phys.*, 2006, vol. 125, p. 014702.
39. Robinson, G.W., Singh, S., Zhu, S.B., and Evans, M.W., *Water in Biology, Chemistry and Physics: Experimental Overviews and Computational Methodologies*, Singapore: World Scientific, 1996.
40. Chen, F. and Smith, P.E., *J. Chem. Phys.*, 2007, vol. 126, p. 221101.
41. Alder, B.J. and Wainwright, T.E., *J. Chem. Phys.*, 1957, vol. 27, p. 1208.

Translated by A. Kirilin